



OPEN

SUBJECT AREAS:

GENETIC VECTORS
METABOLIC DISORDERS
GENETIC TRANSDUCTIONReceived
4 March 2014Accepted
9 June 2014Published
1 July 2014Correspondence and
requests for materials
should be addressed to
T.S. (tshimada@nms.
ac.jp)

Targeted gene transfer into ependymal cells through intraventricular injection of AAV1 vector and long-term enzyme replacement via the CSF

Yoshiyuki Yamazaki, Yukihiko Hirai, Koichi Miyake & Takashi Shimada

Department of Biochemistry and Molecular Biology, Division of Gene Therapy Research Center for Advanced Medical Technology, Nippon Medical School, Bunkyo-ku, Tokyo, Japan.

Enzyme replacement via the cerebrospinal fluid (CSF) has been shown to ameliorate neurological symptoms in model animals with neuropathic metabolic disorders. Gene therapy via the CSF offers a means to achieve a long-term sustainable supply of therapeutic proteins within the central nervous system (CNS) by setting up a continuous source of transgenic products. In the present study, a serotype 1 adeno-associated virus (AAV1) vector was injected into a lateral cerebral ventricle in adult mice to transduce the gene encoding human lysosomal enzyme arylsulfatase A (hASA) into the cells of the CNS. Widespread transduction and stable expression of hASA in the choroid plexus and ependymal cells was observed throughout the ventricles for more than 1 year after vector injection. Although humoral immunity to hASA developed after 6 weeks, which diminished the hASA levels detected in CSF from AAV1-injected mice, hASA levels in CSF were maintained for at least 12 weeks when the mice were tolerized to hASA prior of vector injection. Our results suggest that the cells lining the ventricles could potentially serve as a biological reservoir for long-term continuous secretion of lysosomal enzymes into the CSF following intracerebroventricular injection of an AAV1 vector.

Lysosomal storage disease (LSD) is a diverse group of genetic disorders characterized by an inherited deficiency in specific lysosomal enzymes and a consequent accumulation of undigested substances within lysosomes. Some LSDs have been successfully treated using systemic enzyme replacement therapy (ERT)¹. With that therapy, intravenously delivered lysosomal enzymes are taken up by the target cells via the mannose-6-phosphate receptor-mediated pathway and cross-correct the enzyme deficiency². However, the clinical efficacy of ERT for LSD with neurological symptoms, such as type 3 Gaucher disease and metachromatic leukodystrophy (MLD), is very limited^{3,4}, as lysosomal enzymes cannot cross the blood-brain barrier (BBB)⁵. Thus, alternative drug delivery strategies that circumvent the BBB will be required to treat the central nervous system (CNS) manifestations of LSD.

One possible approach to delivering therapeutic proteins to the CNS is direct injection of a viral vector into the brain parenchyma. We previously showed that in MLD model mice lacking the lysosomal enzyme arylsulfatase A (ASA), a single injection of serotype 1 adeno-associated virus (AAV1) vector encoding human ASA (hASA) into the hippocampus leads to widely distributed expression of hASA protein and a subsequent reduction in sulfatide levels throughout the brain⁶. To apply this approach to large animals, including humans, multiple vector injections with invasive surgical trepanation of the skull is required because the volume of the adult human brain is supposed to be around 3,000 times greater than that of the adult mouse. So far, clinical trials for AAV-mediated treatment of Canavan's disease⁷, Batten's disease⁸ (ClinicalTrials.gov identifier: NCT00151216 and NCT01161576) and Sanfilippo A syndrome (ClinicalTrials.gov identifier: NCT01474343) have been performed or are ongoing. In these studies, the vector is administered through multiple surgical burr holes, but the efficacy of these treatments has been somewhat equivocal.

Another approach is enzyme replacement via the cerebrospinal fluid (CSF), which enhances the enzyme's distribution within the CNS. Repeated or continuous infusion of recombinant protein through intrathecal or intraventricular delivery has been shown to improve neurological symptoms in model animals with neuropathic LSDs^{9–11}. However, repeated lumbar puncture and intrathecal catheter insertion, both of which are considered

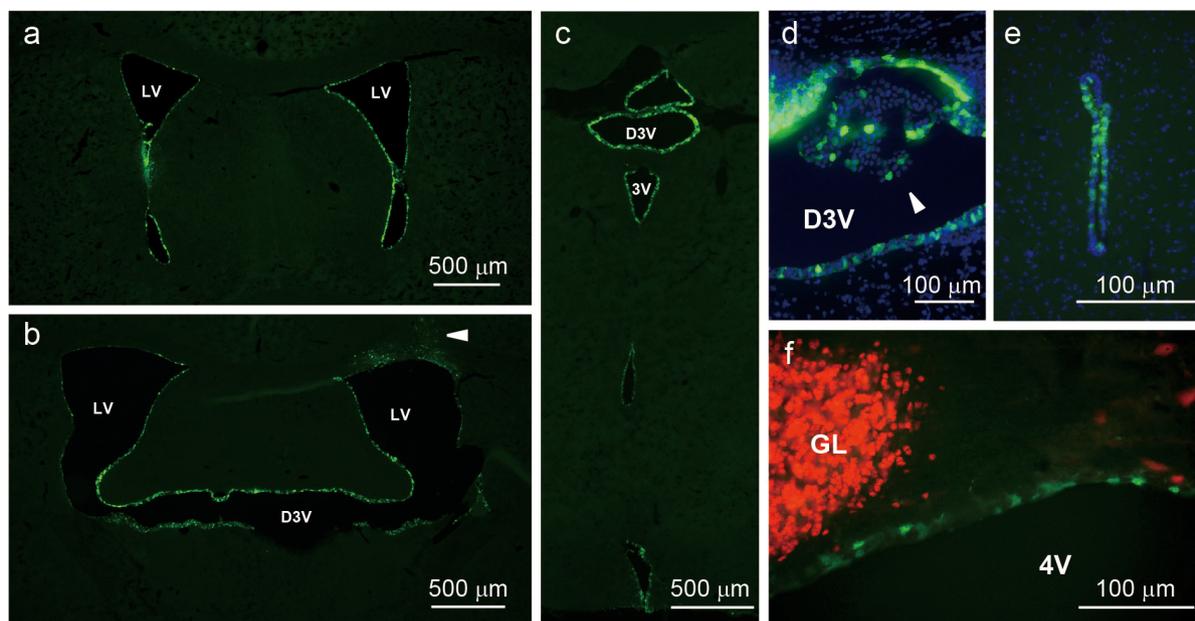


Figure 1 | Transgene expression in coronal sections of mouse brain 3 weeks after injection of bicistronic AAV1 vector into the right lateral ventricle. The injection needle track is indicated with an arrowhead in b. (a–c) Low magnification photomicrographs showing GFP expression in the ependymal cells throughout the right and left lateral ventricles (LV) as well as the dorsal (D3V) and main (3V) parts of the third ventricles. Distances from bregma are 0.08 mm anterior (a), 0.40 mm posterior (b) and 2.32 mm posterior (c), respectively. (d–f) Higher magnification micrographs showing GFP expression in the choroid plexus (arrowhead in d) and the ependymal cells lining the D3V (d), cerebral aqueduct (e) and fourth ventricle (4V) (f). Cell nuclei are stained with DAPI (blue) and neurons in the granular layer (GL) in the cerebellum are labeled with anti-NeuN antibody (red). Distances from bregma are 0.88 (d), 3.28 (e) and 6.16 (f) mm posterior, respectively.

minimally invasive, would likely become unacceptably invasive and expensive for patients who had to continue the regular administration of enzymes over their entire lifespan. In such cases, brain-directed gene therapy could help to reduce the burden on patients by setting up transduced cells within their CNS to continuously secrete the therapeutic enzymes into the CSF for sustained periods. Our aim in the present study is to assess the feasibility of AAV1-mediated enzyme replacement within the CNS via the CSF.

Results

Injection of AAV1 vectors into the CSF leads to widespread transduction of ventricular ependymal cells. To evaluate the feasibility of AAV1-mediated enzyme replacement via the CSF, we first examined the transgene distribution in mouse brain following intracerebroventricular injection of AAV1 bicistronic vectors encoding green fluorescence protein (GFP) and hASA. Immunohistochemical analysis showed that 3 weeks after a single injection of the AAV1 vector into the CSF, GFP expression was broadly distributed in the choroid plexus and ependymal cells throughout the cerebral ventricles (Figure 1). Coronal brain sections revealed the widespread diffusion of AAV1 vectors from the injection site to the contralateral, anterior lateral (Figure 1a, 1b) and third (Figure 1c, 1d) ventricles, as well as fourth ventricles via the cerebral aqueduct (Figure 1e, 1f). GFP expression was mainly confined to the choroid plexus and ependymal cells, with little or no detection in the brain parenchyma or spinal cord. The transduction of ependymal cells was confirmed using an anti-vimentin antibody as a marker of the ependymal cell layer (Figure 2a). Moreover, co-immunostaining of GFP and hASA validated the concurrent expression of these two proteins in same ependymal cells (Figure 2a, 2b). On the other hand, the distribution of these proteins within the cells differed considerably. Whereas GFP was uniformly distributed throughout each cell, the staining pattern of hASA showed a granular distribution surrounding the nucleus (Figure 2b), which suggests transport of the human lysosomal protein into the murine lysosomes. Double

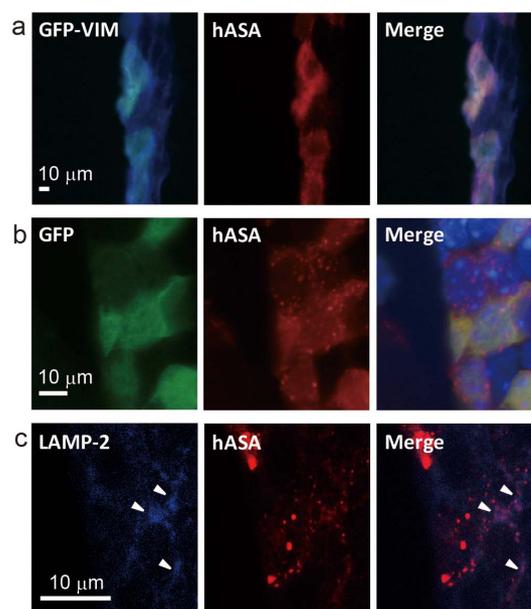


Figure 2 | Concurrent expression and distribution of transduced GFP and hASA within ependymal cells. (a) Co-immunostaining showing that GFP-positive cells (green) are in the ependymal layer and are also stained with anti-vimentin (blue), and that hASA (red) is concurrently expressed in the GFP-positive cells. (b) Higher magnification micrographs showing that GFP is relatively uniformly distributed within ependymal cells, while hASA exhibits more granular localization surrounding the DAPI-stained (blue) cell nuclei. (c) LAMP-2-positivity (blue) confirmed that the transduced hASA is mainly localized in the lysosomes.

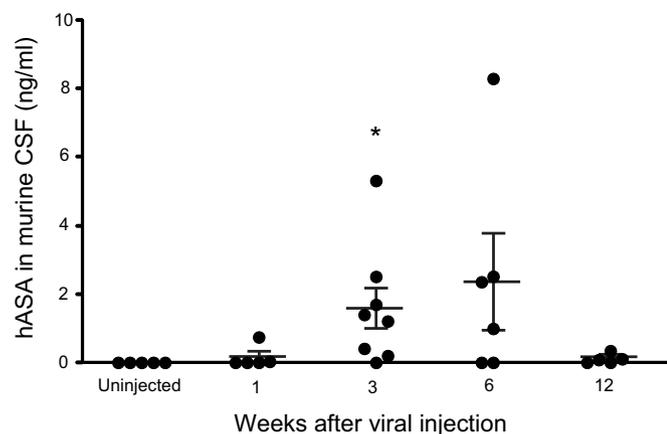


Figure 3 | Time-dependent changes in hASA levels in CSF following AAV1 injection. Each CSF sample was collected from a different mouse at the indicated times. Error bars indicate SEM values. The asterisk indicates a significant difference from uninjected mice (* $P < 0.05$, Mann-Whitney test).

staining of hASA and the lysosomal marker LAMP-2 confirmed the localization of hASA in the lysosomes (Figure 2c).

Secretion of hASA into the CSF and the inhibitory effect of humoral immunity. We next assessed the secretion of hASA from the transduced cells into the CSF of mice. CSF samples collected from the cisterna magna of both AAV1-injected and uninjected mice were assayed for their hASA content using an enzyme-linked immunosorbent assay (ELISA, Figure 3). This confirmed the absence of hASA in CSF from uninjected control mice ($n = 5$). By contrast, in the AAV1-injected mice the average hASA levels in the CSF increased gradually during the period from 1 to 6 weeks after injection (0.15 ± 0.15 ng/ml at 1 week ($n = 5$), 1.59 ± 0.61 ng/ml at 3 weeks ($n = 8$) and 2.36 ± 1.42 ng/ml at 6 weeks ($n = 6$)), but levels had returned nearly to zero by 12 weeks after injection (0.13 ± 0.06 ng/ml ($n = 5$)), indicating that a net peak of the expression of hASA in the CSF has been between 3 and 12 weeks after viral injection. Using a nonparametric rank test because of the zero concentrations in 2 of the 6 samples, a significant difference between AAV1-injected mice and their uninjected counterparts was detected 3 weeks after injection, but not 6 weeks after. In addition, no hASA was detected in the plasma samples collected at same time as the CSF in any of the mice used in this study (data not shown).

To determine why hASA levels in CSF declined within 12 weeks after AAV1 injection, we used immunohistochemical analysis to examine the time course of hASA expression in the brain. Consistent with the results of the ELISA, brain sections from uninjected mice showed no hASA immunoreactivity (Figure 4a, 4d), while hASA expression in the AAV1-injected brains appeared to increase gradually over the period from 1 to 6 weeks after injection (Figure 4b, 4c, 4e–g, 4j). In sharp contrast to the levels in CSF, however, substantial expression of hASA was observed in the brain at 12 weeks after AAV1 injection (Figure 4h, 4k), and could still be seen more than a year post-injection (Figure 4i, 4l). These observations confirm that long-term stable expression of the hASA transgene in the brain can be achieved with the method used here, with no activation of cellular immunity or cellular turnover.

To clarify the reason why hASA levels in CSF were suppressed despite robust expression of the protein, we estimated the effect of humoral immunity by using an immunoprecipitation method to measure the time-dependent development of an anti-hASA antibody. Blood plasma samples collected from AAV1-injected mice at the same time as CSF collection were diluted serially, incubated with

hASA and immunoprecipitated to determine the time-dependent variation in the antibody titer to hASA. Both the averaged (Figure 5a) and individual (Figure 5b) titers showed a significant increase between 3 and 12 weeks after AAV1 injection. From this finding, we would expect a negative correlation between measured concentrations of hASA in CSF and the anti-hASA antibody titers in the AAV1-injected mice.

Long-term replacement of hASA in murine CSF is achieved in immunotolerized animals. To further characterize the effect of antibody development on hASA levels in CSF, we induced C57BL/6 mice to develop tolerance to hASA (Figure 6a). When neonatal mice were intraperitoneally administered $10 \mu\text{g}$ of hASA 30–40 h and then 5 days after birth, subsequent immunoprecipitation analysis of plasma samples showed suppression of antibody development (Figure 6b, 6c), as comparing to untreated mice (Figure 5). Although the immunotolerization protocol did not produce complete tolerance in all treated animals, significant antibody development was suppressed during the 12 weeks after AAV1 injection (Figure 6c).

Using the tolerized mice, we were able to achieve long-term hASA replacement via the CSF (Figure 6d). We confirmed that whereas hASA was not detected in CSF from untreated tolerized mice ($n = 4$), substantial levels were present in CSF from AAV1-injected tolerized mice, with significant increases detected at 6 and 12 weeks (0.43 ± 0.27 ng/ml at 3 weeks ($n = 3$), 2.13 ± 0.39 ng/ml at 6 weeks ($n = 4$) and 2.37 ± 1.27 ng/ml at 12 weeks ($n = 5$)). At 12 weeks, moreover, hASA levels were significantly higher in CSF from tolerized mice than from non-tolerized mice (compare Figure 6d and 3; $P < 0.01$, Mann-Whitney test). These results suggest that AAV1-mediated long-term enzyme replacement via the CSF is feasible under conditions in which humoral immunity does not neutralize the enzyme secreted from the transduced cells. The involvement of an antibody in the inhibition of hASA in CSF was also apparent when the hASA concentration in CSF was plotted against the anti-hASA antibody titer in the plasma of AAV1-injected mice (Figure 7).

Discussion

Ependymal cells have been the preferred target in several gene therapy studies because they are susceptible to a variety of viral vectors and could potentially serve as a reservoir of therapeutic protein that is continuously released into the CSF circulating throughout the brain^{12–18}. Protein secretion from ependymal cells could be especially useful for treatment of LSDs with CNS manifestations, as lysosomal enzymes released into the CSF would be taken up by CNS cells through mannose-6-phosphate receptor-mediated endocytosis. In the present study, we observed that a single intracerebroventricular injection of AAV1 vector induces transgene expression in ependymal cells that persists for more than a year, and that human lysosomal enzymes will continue to be present in the murine CSF in the absence of antibody against the transgene product.

At the microscopic level, intracerebroventricular injection of AAV1 vector showed exclusive transduction of ependymal cells lining the ventricles and the choroid plexus forming the blood-CSF barrier (Figure 1 and 4). This is similar to the transduction pattern seen after intracerebroventricular injection of other serotypes of AAV^{15,19} or adenoviral vector^{12–14}. Although AAV1 vector has been reported to achieve broader neuronal transduction if they were injected into the lateral ventricles of neonatal mouse²⁰, matured ependymal cells would prevent their transfer from the CSF to the brain parenchyma in adult mice because the maturation of ependymal cells occurs during the first postnatal week²¹. In earlier studies, it was reported that some ependymal cells behave as stem cells, even in the adult mouse²², and that ependymal cells turn approximately every 130 days²³. In a more recent study, however, ependymal cells were reportedly quiescent under normal conditions (i.e., in the

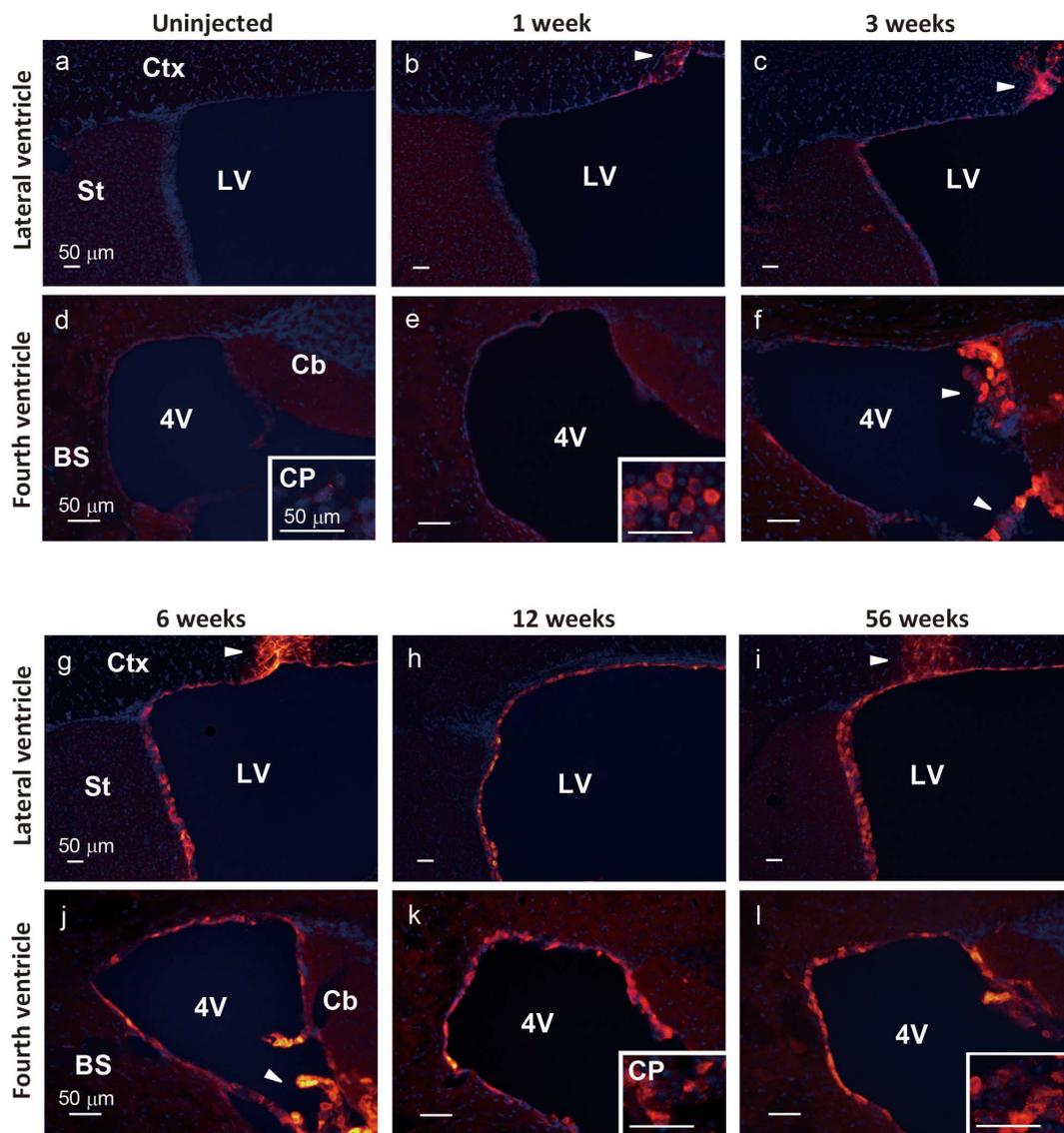


Figure 4 | Time-dependent changes in expression levels of transduced hASA in the brain. Expression patterns of AAV1-transduced hASA (red) in the LV (a–c and g–i) and 4V (d–f and e–l) are shown at the indicated pre- and post-injection times. The injection needle tracks are indicated by arrowheads in (b), (c), (g) and (i). Cell nuclei are stained with DAPI (blue). Immunohistochemical staining showed no hASA signal anywhere in the brain of an uninjected control mouse (a, d), though a weak false-positive signal was detected in the choroid plexus (inset in (d)). One week after injection, overt signals could be seen in the cortical cells surrounding the needle track (arrowhead in (b)) and in the choroid plexus (inset in (e)), but there were very few hASA-expressing ventricular ependymal cells (b, e). Three weeks after injection, hASA-positive ependymal cells were sparsely distributed throughout the ventricles (c, f), and the choroid plexus (arrowheads in (f)) was densely stained. Six weeks after injection, stable expression of hASA could be seen in both ventricular ependymal cells (g–l) and choroid plexus (arrowhead in (j) and insets in (k) and (l)), and that expression persisted for over 1 year. BS, brain stem; Cb, cerebellum; CP, choroid plexus; Ctx, cortex; St, striatum.

absence of brain injury) by virtue of Notch signal activation²⁴. In fact, intracerebroventricular injection of a helper-dependent adenoviral vector, which does not induce cellular immunity, led to expression of the transgene for up to 1 year in ependymal cells expressing Notch1¹². Similarly, we observed stable expression of human lysosomal enzymes in murine ependymal cells over more than 1 year (Figure 4), which suggests the AAV1 vector has a high affinity for quiescent ependymal cells and is indicative of the suitability of the method used in the present study to set up a continuous source of lysosomal enzymes to be released into the CSF.

To estimate the amount of human enzyme secreted into the CSF of mice, we used a glass capillary tube to collect CSF samples from the cisterna magna as described previously²⁵ and measured the hASA concentration using a traditional ELISA. Although we visually confirmed that there was no contamination of the collected CSF by

blood, we would expect small amounts of blood to have little or no effect on the estimated concentrations of hASA in CSF, as hASA was not detected in any blood samples collected simultaneously with the CSF (data not shown). Considering that CSF ultimately drains into the bloodstream and lymphatics²⁶, it is somewhat surprising that we did not detect hASA in blood samples from the tolerized mice, in which anti-hASA antibody titers were suppressed. We suggest that the hASA concentration in the blood plasma was diluted to a level below the detection limit of our assay due to the difference between the total volumes of CSF (approximately 40 μ l)²⁷ and plasma (at least more than 1.2 ml)²⁸. We also did not detect cells expressing hASA in the livers of the AAV1-injected mice (data not shown). Most likely, therefore, an anti-hASA antibody developed in the blood in response to hASA draining from the brain, not in response to hASA secreted from infected cells outside the CNS. Although we could not directly

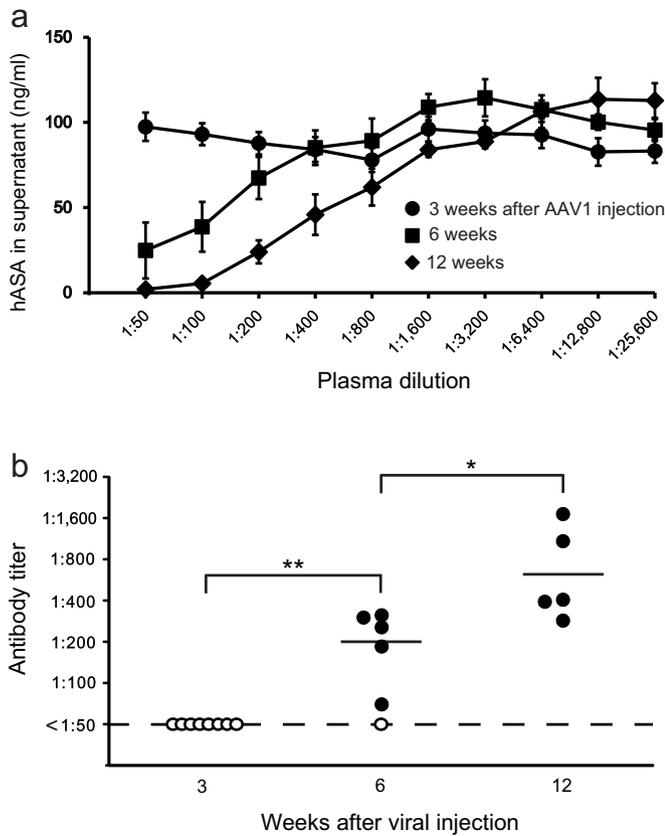


Figure 5 | Development of anti-hASA antibody titers in plasma from AAV1-injected mice. (a) Aliquots (2 μ l) of plasma collected 3 weeks (circles, $n = 8$), 6 weeks (squares, $n = 6$) and 12 weeks (diamonds, $n = 5$) after AAV1 injection were serially diluted two-fold and added to a fixed amount of hASA to form IgG-hASA complexes. The immune complexes were then precipitated, and the residual hASA concentration in the supernatant was measured to evaluate the plasma's ability to capture hASA. Data points represent average values for each group, and the error bars indicate SEM values. (b) The antibody titers in individuals (closed circles) were determined from the half-maximal value of each individual dilution curve. The dotted horizontal line indicates the antibody titer detection limit, and the data under this line (open circles) were excluded from the calculation to find the average. The short solid horizontal lines represent the average values of the detectable titers in the two groups (3 and 6 weeks after injection). During the periods spanning from 3 to 6 weeks and from 6 to 12 weeks after injection, antibody titers in each group increased significantly (* $P < 0.05$; ** $P < 0.01$, Mann-Whitney test).

determine antibody titers in CSF due to the small volume of the CSF samples and the very low concentration of the anti-hASA IgG, the time course of antibody development in the CSF would be coincident with that in the plasma, since IgG present in the bloodstream can rapidly cross the BBB via receptor-mediated transcytotic pathways^{5,29}.

Evidence from several animal LSD models with CNS manifestations suggests treatments that raise levels of lysosomal enzymes in CSF have a potential for clinical use^{9–11}. For example, intracerebroventricular administration of hASA to MLD model mice using osmotic minipumps improved motor function and reduced sulfatide accumulation in the CNS, but did not elicit detectable anti-hASA antibodies during the 4 weeks of treatment¹⁰. In our study, however, significant development of anti-hASA antibodies was observed 12 weeks after AAV injection and likely had a negative relationship with the measured level of hASA in the CSF (Figure 7). That hASA levels could not be sustained in the long term in the CSF of immunocompetent wild-type mice (Figure 3) indicates development of humoral immunity will be a key obstacle to the widespread use of the method

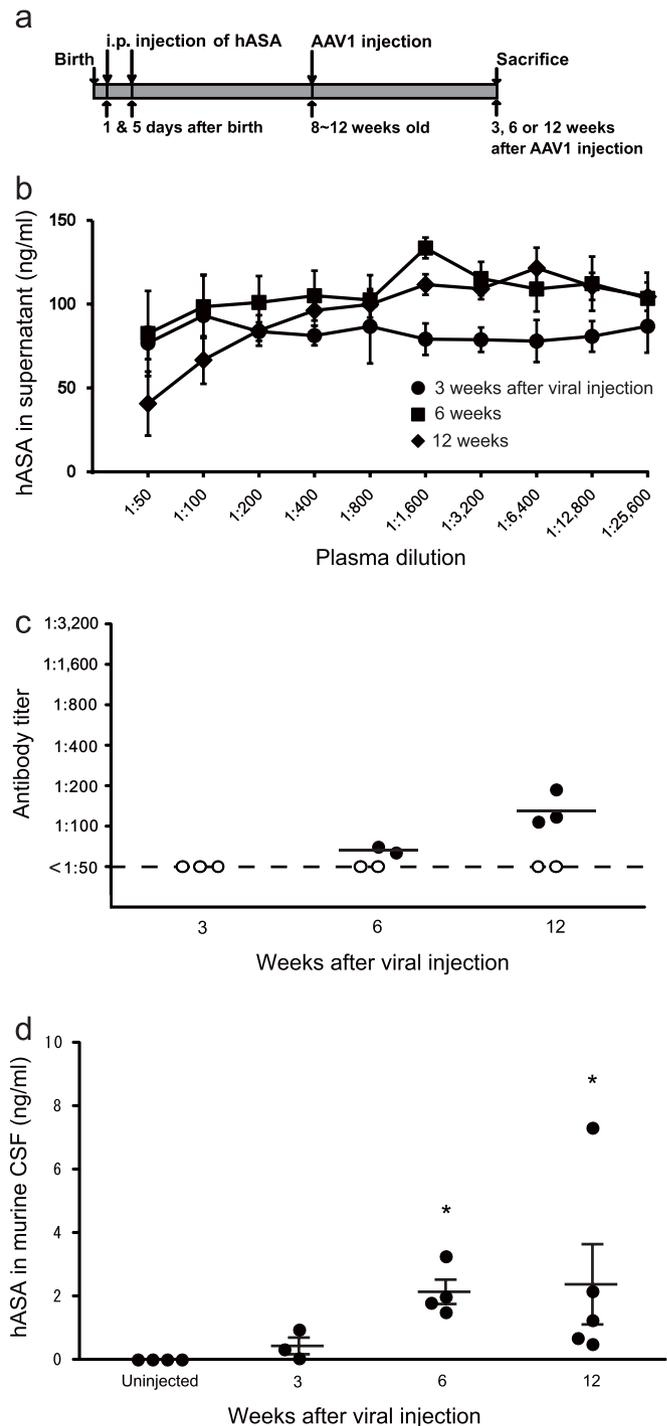


Figure 6 | Long-term enzyme replacement via the CSF in mice tolerized to hASA. (a) Illustration of the experimental timeline. To induce tolerance to hASA, neonatal C57BL/6 mice were intraperitoneally injected with 10 μ g of hASA 30–40 h and 5 days after birth. (b) Two microliters of plasma were then taken from the immunotolerized mice 3 weeks (circles, $n = 3$), 6 weeks (squares, $n = 4$) and 12 weeks (diamonds, $n = 5$) after hASA injection. All other details are the same as in Figure 5. (c) The antibody titer in the individuals. Details are same as in Figure 5. There were no significant differences among the three groups (Kruskal-Wallis test: $H = 3.20$, $P = 0.20$). (d) Time-dependent changes in hASA levels in CSF. Asterisks indicate significant differences from uninjected mice (* $P < 0.05$, Mann-Whitney test).

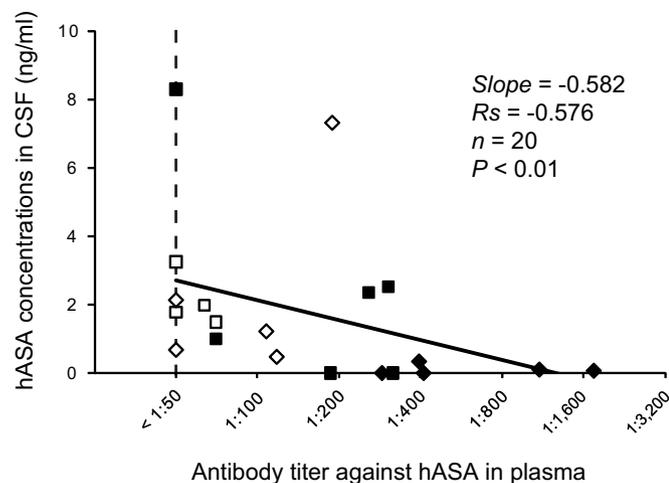


Figure 7 | Negative correlations between measured concentrations of hASA in CSF and anti-hASA antibody titers in plasma from injected mice. Closed squares ($n = 6$) and diamonds ($n = 5$) depict results from immunocompetent mice 6 and 12 weeks after injection, respectively (same samples shown in Figure 3 and 5b). Open squares ($n = 4$) and diamonds ($n = 5$) indicate results from immunotolerized mice 6 and 12 weeks after injection, respectively (same samples shown in Figure 6c and d). The dotted vertical line indicates the antibody titer detection limit. The correlation between the hASA level in CSF and the anti-hASA antibody titers was significant with a negative slope. R_s = Spearman's rank correlation coefficient.

employed here. On the other hand, because most MLD patients express mutant hASA that lacks normal functionality but contains polypeptides that could potentially confer immunological tolerance to the substituted normal hASA³⁰, increased CSF levels of human lysosomal enzymes could have benefits in human patients that are not seen in animal models, as was suggested in earlier ERT studies^{31,32}. In addition, another immune problem which was not appeared in the rodent study will be faced with regard to the clinical trials using AAV1 vector. As a majority of healthy human population has been reported to be seropositive for neutralizing antibodies (NABs) to AAV1³³, it seems that AAV1 would be neutralized immediately in the majority of human patients. However, recent study has reported that intra-CSF delivered AAV vector attained the gene transfer to the canine CNS even in the presence of NABs in the serum of treating animals because the NABs titers in the CSF was much lower than that in the serum and thus did not completely block AAV vector transduction in the brain³⁴. Considering this report, intracerebroventricular administration of AAV1 vector could have benefit to circumvent not only the BBB but also the immune response against the AAV capsid.

We previously reported that intrahippocampal injection of an AAV1 vector encoding hASA reduced sulfatide levels throughout the entire brain and improved motor function in MLD model mice⁶. We are now investigating using this MLD model mice if there is any beneficial metabolic effect by our intracerebroventricular injection protocol with AAV1 vector. Although we cannot compare the CSF level of hASA which was achieved in this study with that of murine hASA in the normal mice because of a lack of the information about the murine hASA level in the normal mice, our next therapeutic study will reveal whether the CSF level of hASA that will be achieved by our protocol is enough to improve the MLD symptoms or not. Furthermore, in larger animals, gene therapy via the ependymal route would be a more effective means of delivering lysosomal enzymes to the entire brain, as CSF flows not only through the cerebral ventricles and the subarachnoid space but also the perivascular space and the brain parenchyma³⁵. In future studies, we will test

whether the method used here in mice is able to provide the same results in larger animals with larger brains, where diffusion distances and the CSF volume to be loaded with therapeutic proteins are much greater.

Methods

AAV vector preparation. The AAV vector plasmid used here (pAAV.CAhASABE) was as described previously^{6,36}. To generate the AAV1 vector, an adenovirus-free triple transfection method was performed as described previously^{6,36,37}. To remove residual hASA proteins from the obtained AAV1 vector solution prior to animal injection, size-exclusion chromatography was performed using an AKTA Explorer 100 HPLC system (GE Healthcare Japan, Tokyo, Japan) as described previously^{37,38}. The absence of detectable hASA contamination in the AAV1 vector solution was then confirmed using an ELISA (see below). The AAV1 titer was determined by quantitative real-time polymerase chain reaction using SYBR Premix Ex Taq (Takara Bio, Shiga, Japan) after purification through phenol-chloroform extraction³⁸.

Animals and injections. All animal experiments were approved by the Ethics Committee of Nippon Medical School and carried out according to the Institutional guidelines for animal care (Nippon Medical School, Tokyo, Japan). Eight- to 12-week-old C57BL/6 mice (Saitama Experimental Animal Supply Co., Saitama, Japan) were used in this study. All mice used here were healthy wild-type mice. To reduce the effect of antibody development against hASA in the AAV1 injected animals, C57BL/6 mice were immunotolerized to hASA using a published protocol in which neonatal mice were intraperitoneally injected with 10 μ g of enzyme protein 30–40 h and 5 days after birth to induce tolerance³⁹. To administer the vector, the mice were initially anesthetized with sodium pentobarbital (40 mg/kg) and then mounted on a stereotaxic frame. The skin over the skull was incised and a small hole was made in the skull above the target using a microdrill. The injection site was the right lateral ventricle, and the stereotaxic brain coordinates were 0.4 mm posterior, 1.0 mm lateral and 3 mm deep from bregma. Twenty microliters of AAV1 vector solution (approximately 1×10^{13} vg/ml) were delivered over a period of 10 min using a syringe with a thick needle (Ito Co., Shizuoka, Japan). Following injection, the needle was left in place for 10 min to allow the injected solution to diffuse into the CSF prior to withdrawal.

Collection of CSF and blood. At various times after injection, mice were deeply anesthetized and transcardially perfused with 0.1 M phosphate-buffered saline (PBS) followed by 4% paraformaldehyde. Prior to perfusion, CSF samples were taken from the cisterna magna using a puncture technique reported previously²⁵, and blood was collected by cardiac puncture. The volume of CSF and blood obtained from each mouse was 4–10 μ l and 400–500 μ l, respectively. CSF samples with visible blood contamination were discarded. Whole blood was treated with heparin and centrifuged for 30 min at 3,000 rpm at room temperature, and the resulting supernatant was recovered as plasma.

Histology. After the perfusion fixation, the brains were dissected out and postfixed overnight in 4% paraformaldehyde at 4°C before being immersed in PBS containing 30% sucrose for cryoprotection. Brain sections were then cut to a thickness of 20 μ m using a freezing sliding microtome. For histological analyses, free-floating sections were washed in PBS and then blocked for 1 h in 1% skim milk (Nacalai Tesque, Kyoto, Japan) in PBS. Immunostaining for hASA and GFP was performed using anti-hASA goat IgG (R&D Systems, Minneapolis, MN; dilution 1:100) and anti-GFP rabbit IgG (MBL International Co., Woburn, MA; dilution 1:500) as primary antibodies. To identify cellular structures, anti-vimentin mouse IgG (Dako Japan, Kyoto, Japan; dilution 1:50) and anti-LAMP-2 rat IgG (Santa Cruz Biotechnology, Santa Cruz, CA; dilution 1:50) were also used. The brain sections were incubated overnight with one or two types of primary antibody diluted in PBS with 0.1% Triton X-100 at 4°C, then washed in PBS 3 times for 5 min each at room temperature. Thereafter, they were incubated for 2 h at room temperature with a fluorescent secondary antibody and/or a biotinylated secondary antibody. Biotinylated samples were then incubated with a streptavidin-conjugated fluorochrome for 1 h at room temperature. The secondary antibodies used were Alexa350- and Alexa488-conjugated anti-rat and anti-rabbit IgG (Life Technologies Japan, Tokyo, Japan; dilution 1:100) and biotinylated anti-goat IgG (Vector Laboratories, Burlingame, CA; dilution 1:100). The streptavidin-conjugated fluorochrome used was Alexa555 (Life Technologies Japan, Tokyo, Japan; dilution 1:100). After the sections were mounted and coverslipped, fluorescent signals were imaged using a BX-60 fluorescence microscope (Olympus, Tokyo, Japan) and a TCS SP5 confocal microscope (Leica Microsystems, Tokyo, Japan).

Biochemical analysis. hASA concentrations in CSF and blood samples were determined using an indirect sandwich ELISA, as described previously³⁶. Although 86% of all amino acids are conserved between mouse and human hASA⁴⁰, with the anti-hASA antibodies used in this study, no cross-reactivity was observed with samples taken from untreated mice expressing their own murine hASA (see Figure 3). This is indicative of the high specificity of the antibody for the human protein. For the ELISA, 4 μ l of CSF gave a satisfactory result at 1:15 dilution. No hASA was detected in blood samples from AAV1-injected mice (data not shown).



The titer of anti-hASA antibody developed in AAV1-injected mice was determined by measuring the capacity of a twofold dilution series of 2- μ l aliquots of plasma to immunoprecipitate hASA, as described previously⁴¹. The value of the titer described in this report represents the calculated plasma dilution at a turning point in the sigmoid function, which was fitted to the dilution curve obtained experimentally.

Statistics. Data from experiments are expressed as means \pm SEM. Each data set was treated statistically as described in the individual figure legends. An error level of 5% ($P < 0.05$) was considered significant.

- Beck, M. Therapy for lysosomal storage disorders. *IUBMB Life* **62**, 33–40 (2010).
- Braulke, T. & Bonifacino, J. S. Sorting of lysosomal proteins. *Biochim Biophys Acta* **1793**, 605–614 (2009).
- Vellodi, A. *et al.* Management of neuronopathic Gaucher disease: revised recommendations. *J Inherit Metab Dis* **32**, 660–664 (2009).
- i Dali, C. & Lund, A. M. in *ACMG Meeting* (2009).
- Begley, D. J., Pontikis, C. C. & Scarpa, M. Lysosomal storage diseases and the blood-brain barrier. *Curr Pharm Des* **14**, 1566–1580 (2008).
- Kurai, T. *et al.* AAV1 mediated co-expression of formylglycine-generating enzyme and arylsulfatase efficiently corrects sulfatide storage in a mouse model of metachromatic leukodystrophy. *Mol Ther* **15**, 38–43 (2007).
- McPhee, S. W. *et al.* Immune responses to AAV in a phase I study for Canavan disease. *J Gene Med* **8**, 577–588 (2006).
- Worgall, S. *et al.* Treatment of late infantile neuronal ceroid lipofuscinosis by CNS administration of a serotype 2 adeno-associated virus expressing CLN2 cDNA. *Hum Gene Ther* **19**, 463–474 (2008).
- Crawley, A. C. *et al.* Enzyme replacement reduces neuropathology in MPS IIIA dogs. *Neurobiol Dis* **43**, 422–434 (2011).
- Stroobants, S. *et al.* Intracerebroventricular enzyme infusion corrects central nervous system pathology and dysfunction in a mouse model of metachromatic leukodystrophy. *Hum Mol Genet* **20**, 2760–2769 (2011).
- Calias, P. *et al.* CNS penetration of intrathecal-lumbar idursulfase in the monkey, dog and mouse: implications for neurological outcomes of lysosomal storage disorder. *PLoS One* **7**, e30341 (2012).
- Dindot, S., Piccolo, P., Grove, N., Palmer, D. & Brunetti-Pierri, N. Intrathecal injection of helper-dependent adenoviral vectors results in long-term transgene expression in neuroependymal cells and neurons. *Hum Gene Ther* **22**, 745–751 (2011).
- Nishida, F. *et al.* Restorative effect of intracerebroventricular insulin-like growth factor-I gene therapy on motor performance in aging rats. *Neuroscience* **177**, 195–206 (2011).
- Hereñú, C. B., Sonntag, W. E., Morel, G. R., Portiansky, E. L. & Goya, R. G. The ependymal route for insulin-like growth factor-1 gene therapy in the brain. *Neuroscience* **163**, 442–447 (2009).
- Liu, G., Martins, I. H., Chiorini, J. A. & Davidson, B. L. Adeno-associated virus type 4 (AAV4) targets ependyma and astrocytes in the subventricular zone and RMS. *Gene Ther* **12**, 1503–1508 (2005).
- Liu, G., Martins, I., Wemmie, J. A., Chiorini, J. A. & Davidson, B. L. Functional correction of CNS phenotypes in a lysosomal storage disease model using adeno-associated virus type 4 vectors. *J Neurosci* **25**, 9321–9327 (2005).
- Benraiss, A. *et al.* Sustained induction of neuronal addition to the adult rat neostriatum by AAV4-delivered noggin and BDNF. *Gene Ther* **19**, 483–493 (2012).
- Dodge, J. C. *et al.* AAV4-mediated expression of IGF-1 and VEGF within cellular components of the ventricular system improves survival outcome in familial ALS mice. *Mol Ther* **18**, 2075–2084 (2010).
- Davidson, B. L. *et al.* Recombinant adeno-associated virus type 2, 4, and 5 vectors: transduction of variant cell types and regions in the mammalian central nervous system. *Proc Natl Acad Sci U S A* **97**, 3428–3432 (2000).
- Passini, M. A. *et al.* Intraventricular brain injection of adeno-associated virus type 1 (AAV1) in neonatal mice results in complementary patterns of neuronal transduction to AAV2 and total long-term correction of storage lesions in the brains of beta-glucuronidase-deficient mice. *Journal of virology* **77**, 7034–7040 (2003).
- Spassky, N. *et al.* Adult ependymal cells are postmitotic and are derived from radial glial cells during embryogenesis. *J Neurosci* **25**, 10–18 (2005).
- Coskun, V. *et al.* CD133+ neural stem cells in the ependyma of mammalian postnatal forebrain. *Proc Natl Acad Sci U S A* **105**, 1026–1031 (2008).
- Chauhan, A. N. & Lewis, P. D. A quantitative study of cell proliferation in ependyma and choroid plexus in the postnatal rat brain. *Neuropathol Appl Neurobiol* **5**, 303–309 (1979).
- Carlén, M. *et al.* Forebrain ependymal cells are Notch-dependent and generate neuroblasts and astrocytes after stroke. *Nat Neurosci* **12**, 259–267 (2009).
- Liu, L. & Duff, K. A technique for serial collection of cerebrospinal fluid from the cisterna magna in mouse. *J Vis Exp* (2008).
- Abbott, N. J. Evidence for bulk flow of brain interstitial fluid: significance for physiology and pathology. *Neurochem Int* **45**, 545–552 (2004).
- Rudick, R. A., Zirretta, D. K. & Herndon, R. M. Clearance of albumin from mouse subarachnoid space: a measure of CSF bulk flow. *J Neurosci Methods* **6**, 253–259 (1982).
- Riches, A. C., Sharp, J. G., Thomas, D. B. & Smith, S. V. Blood volume determination in the mouse. *J Physiol* **228**, 279–284 (1973).
- Zlokovic, B. V. *et al.* A saturable mechanism for transport of immunoglobulin G across the blood-brain barrier of the guinea pig. *Exp Neurol* **107**, 263–270 (1990).
- Polten, A. *et al.* Molecular basis of different forms of metachromatic leukodystrophy. *N Engl J Med* **324**, 18–22 (1991).
- Matzner, U. *et al.* Enzyme replacement improves nervous system pathology and function in a mouse model for metachromatic leukodystrophy. *Hum Mol Genet* **14**, 1139–1152 (2005).
- Matzner, U. *et al.* Induction of tolerance to human arylsulfatase A in a mouse model of metachromatic leukodystrophy. *Mol Med* **13**, 471–479 (2007).
- Boutin, S. *et al.* Prevalence of serum IgG and neutralizing factors against adeno-associated virus (AAV) types 1, 2, 5, 6, 8, and 9 in the healthy population: implications for gene therapy using AAV vectors. *Hum Gene Ther* **21**, 704–712 (2010).
- Haurigot, V. *et al.* Whole body correction of mucopolysaccharidosis IIIA by intracerebrospinal fluid gene therapy. *The Journal of clinical investigation* (2013).
- Iliff, J. J. *et al.* A paravascular pathway facilitates CSF flow through the brain parenchyma and the clearance of interstitial solutes, including amyloid beta. *Sci Transl Med* **4**, 147ra111 (2012).
- Iwamoto, N. *et al.* Global diffuse distribution in the brain and efficient gene delivery to the dorsal root ganglia by intrathecal injection of adeno-associated viral vector serotype 1. *J Gene Med* **11**, 498–505 (2009).
- Miyake, K., Miyake, N., Yamazaki, Y., Shimada, T. & Hirai, Y. Serotype-independent method of recombinant adeno-associated virus (AAV) vector production and purification. *J Nippon Med Sch* **79**, 394–402 (2012).
- Uchida, A. *et al.* Non-human primate model of amyotrophic lateral sclerosis with cytoplasmic mislocalization of TDP-43. *Brain* **135**, 833–846 (2012).
- Golumbeski, G. S., Jr. & Dimond, R. L. The use of tolerization in the production of monoclonal antibodies against minor antigenic determinants. *Anal Biochem* **154**, 373–381 (1986).
- Kreysing, J. *et al.* Structure of the mouse arylsulfatase A gene and cDNA. *Genomics* **19**, 249–256 (1994).
- Matzner, U. *et al.* Non-inhibitory antibodies impede lysosomal storage reduction during enzyme replacement therapy of a lysosomal storage disease. *J Mol Med (Berl)* **86**, 433–442 (2008).

Acknowledgments

The study was done in Tokyo, Japan. This study was supported in part by grants from the Japanese Ministry of Health, Labour and Welfare and Ministry of Education, Culture, Sports, Science and Technology. We thank Guangping Gao and James M. Wilson (University of Pennsylvania, PA) for providing AAV packaging plasmids and Keiya Ozawa (Jichi Medical University, Tochigi, Japan) for providing HEK293 cells.

Author contributions

Y.Y. wrote the main manuscript text and prepared all figures; Y.H. prepared the AAV1 vectors; K.M. supervised the project; T.S. designed research and had primary responsibility for final content.

Additional information

Competing financial interests: The authors declare no competing financial interests.

How to cite this article: Yamazaki, Y., Hirai, Y., Miyake, K. & Shimada, T. Targeted gene transfer into ependymal cells through intraventricular injection of AAV1 vector and long-term enzyme replacement via the CSF. *Sci. Rep.* **4**, 5506; DOI:10.1038/srep05506 (2014).



This work is licensed under a Creative Commons Attribution-NonCommercial-NoDerivs 4.0 International License. The images or other third party material in this article are included in the article's Creative Commons license, unless indicated otherwise in the credit line; if the material is not included under the Creative Commons license, users will need to obtain permission from the license holder in order to reproduce the material. To view a copy of this license, visit <http://creativecommons.org/licenses/by-nc-nd/4.0/>